plants

MDPI

Article

Functional Characterization of Three Diterpene Synthases Responsible for Tetracyclic Diterpene Biosynthesis in *Scoparia dulcis*

Jung-Bum Lee *, Tomoya Ohmura and Yoshimi Yamamura

Graduate School of Medicine and Pharmaceutical Sciences, University of Toyama, 2630 Sugitani, Toyama 930-0194, Japan

* Correspondence: lee@pha.u-toyama.ac.jp; Tel.: +81-76-434-7580

Abstract: *Scoparia dulcis* produces unique biologically active diterpenoids such as scopadulcic acid B (SDB). They are biosynthesized from geranylgeranyl diphosphate (GGPP) via *syn*-copalyl diphosphate (*syn*-CPP) and scopadulanol as an important key intermediate. In this paper, we functionally characterized three diterpene synthases, SdCPS2, SdKSL1 and SdKSL2, from *S. dulcis*. The SdCPS2 catalyzed a cyclization reaction from GGPP to *syn*-CPP, and SdKSL1 did from *syn*-CPP to scopadulan-13α-ol. On the other hand, SdKSL2 was found to incorporate a non-sense mutation at 682. Therefore, we mutated the nucleotide residue from A to G in SdKSL2 to produce SdKSL2mut, and it was able to recover the catalytic function from *syn*-CPP to *syn*-aphidicol-16-ene, the precursor to scopadulin. From our results, SdCPS2 and SdKSL1 might be important key players for SDB biosynthesis in *S. dulcis*.

Keywords: diterpene synthase; *Scoparia dulcis*; cyclase

check for updates

Citation: Lee, J.-B.; Ohmura, T.; Yamamura, Y. Functional Characterization of Three Diterpene Synthases Responsible for Tetracyclic Diterpene Biosynthesis in *Scoparia dulcis*. *Plants* **2023**, *12*, 69. https://doi.org/10.3390/plants12010069

Academic Editor: Juei-Tang Cheng

Received: 16 December 2022
Revised: 21 December 2022
Accepted: 21 December 2022
Published: 23 December 2022

1. Introduction

Plants produce a vast array of secondary metabolites, and these natural products are of increasing importance as a resource for drugs and drug leads. The chemical diversity of natural products is enormous, and is derived from its biosynthetic machinery. Among important natural products, terpenes are the largest group, and they range from simple flavor and fragrance compounds to complex triterpenoids. Large populations of terpenes are cyclic compounds possessing several chiral centers, and the cyclization catalyzed by terpene synthases is the first step in constructing their diverse structures. Scopadulcic acid B (SDB, **1**) is a unique tetracyclic diterpenoid produced by a perennial medicinal herb, *Scoparia dulcis* L. (Plantaginaceae, Lamiales), which is distributed among tropical and subtropical regions [1]. SDB, **1** has attracted substantial attention both for its multiple biological effects and its unique tetracyclic skeleton. Early studies suggested that the SDB biosynthetic process was initiated by two sequential steps: the formation of *syn*-copalyl diphosphate (*syn*-CPP, **3**) from geranylgeranyl diphosphate (GGPP, **2**), and the subsequent cyclization of the tetracyclic skeleton from **3** (Scheme 1). Such dual cyclization schemes are characteristic machinery for the biosynthesis of labdane-related diterpenoids (LRDs) [2,3].

Recently, we have discovered a gene candidates responsible for the biosynthesis of **1** by the RNA-seq analysis of *S. dulcis* [4]. In this study, we describe the characteristics of the key enzymes for unique diterpene biosynthesis in *S. dulcis*.

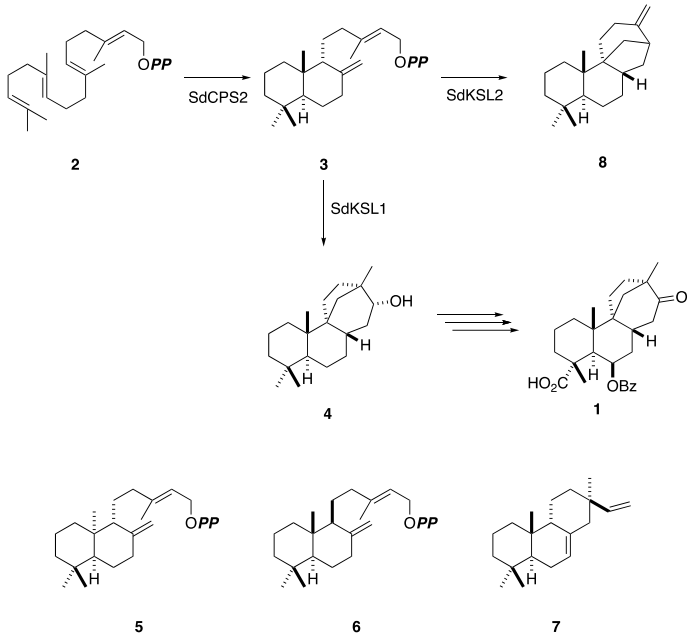

Scheme 1. Proposed biosynthetic pathway of diterpenes in *S. dulcis* and chemical structures of related diterpenes: (**1**) scopadulcic acid B, (**2**) geranylgeranyl diphosphate, (**3**) *syn*-copalyl diphosphate, (**4**) scopadula-13α-ol, (**5**) *ent*-copalyl diphosphate, (**6**) (+)-copalyl diphosphate, (**7**) *syn*-pimara-7,15-diene, (**8**) aphidicol-16-ene.

2. Results

2.1. Cloning of Diterpene Synthases

Gene candidates for unique diterpene synthases (DTSs) were cloned from a cDNA library prepared with *S. dulcis*. Both gene candidates were cloned from the cDNA library prepared with *S. dulcis*. *SdCPS2* (2412 bp) encoded 804 amino-acid residues containing the *N*-terminal transit-peptide sequence. It showed typical features of monofunctional-angiosperm class II diterpene synthases (DTSs) featuring a three-domain structure (γ-β-α). It also included the characteristic DxDD motif, which functions as the general acid to protonate the terminal carbon-carbon double bond of the substrate **2**. In addition, SdCPS2 contained SAYDTAW and QxxDGSW motifs, which are well-conserved in class II DTSs (Figure S1) [5]. The function of the former motif is still unknown, whereas the later motif is proposed to be involved in the stabilization of the intermediate cation during the cyclization. On the other hand, *SdKSL1* (2412 bp) encoded 805 amino acid residues with *N*-terminal transit-peptide sequence. Moreover, SdKSL1 also featured a three-domain structure the same as SdCPS2. SdKSL1, containing the characteristic DDxxD and NSE/DTE motifs for class I DTSs (Figure S1). These conserved motifs are involved in metal-dependent ionization of the prenyl diphosphate substrates. In addition, we cloned another class I DTS gene, *SdKSL2* (2401 bp). The coding sequence (CDS) of *SdKSL2* covered nearly the full length of the gene when compared with those of class I DTSs. It was noteworthy that the CDS introduced a non-sense mutation at 682 position (Figure S1). The identity between SdKSL1 and SdKSL2 was very high (88%).

Homology searches against protein sequences indicated that SdCPS2 showed high identity with functionally annotated *syn*-CPS, VacTPS3 from *Vitex angus-castus* (AUT77122, 63%) [6]. In addition, it is noteworthy that identity against *syn*-CPS from *Oryza sativa* (OsCPS4, BAD42451, 39%) [7] is quite low. On the other hand, SdKSL1 showed extended similarities with already functionally annotated KSLs from *Isodon rubescens* such as IrKSL6 (isopimaradiene synthase, ASC55318, 46%) [8] and IrTPS2 (nezukol synthase, ARO38140, 46%) [9]. So far, VacTPS6 from *V. angus-castus* (*syn*-isopimara-7,15-diene synthase, AUT77125) [6] have been shown to accept *syn*-CPP as a substrate; however, the

identity between SdKSL1 and VacTPS6 was 44%. Finally, SdKSL2 showed the highest identity against putative *cis*-abienol synthase from *Handroanthus impetiginosus* (PIN17551, 50%).

As shown in Figure 1, phylogenetic relationships were found for diterpene synthases. In particular, SdCPS2 was placed into the clade, consisting of class II DTSs responsible for secondary metabolism. It is noteworthy that SdCPS2 was found to be closely related to VacTPS3, which is reported to be a *syn*-copalyl diphosphate synthase. On the other hand, SdKSL1 and SdKSL2 were also placed into the clade consisting of class I DTSs related to the secondary metabolism. Therefore, these three diterpene synthases might be involved in unique diterpene biosynthesis in *S. dulcis*.

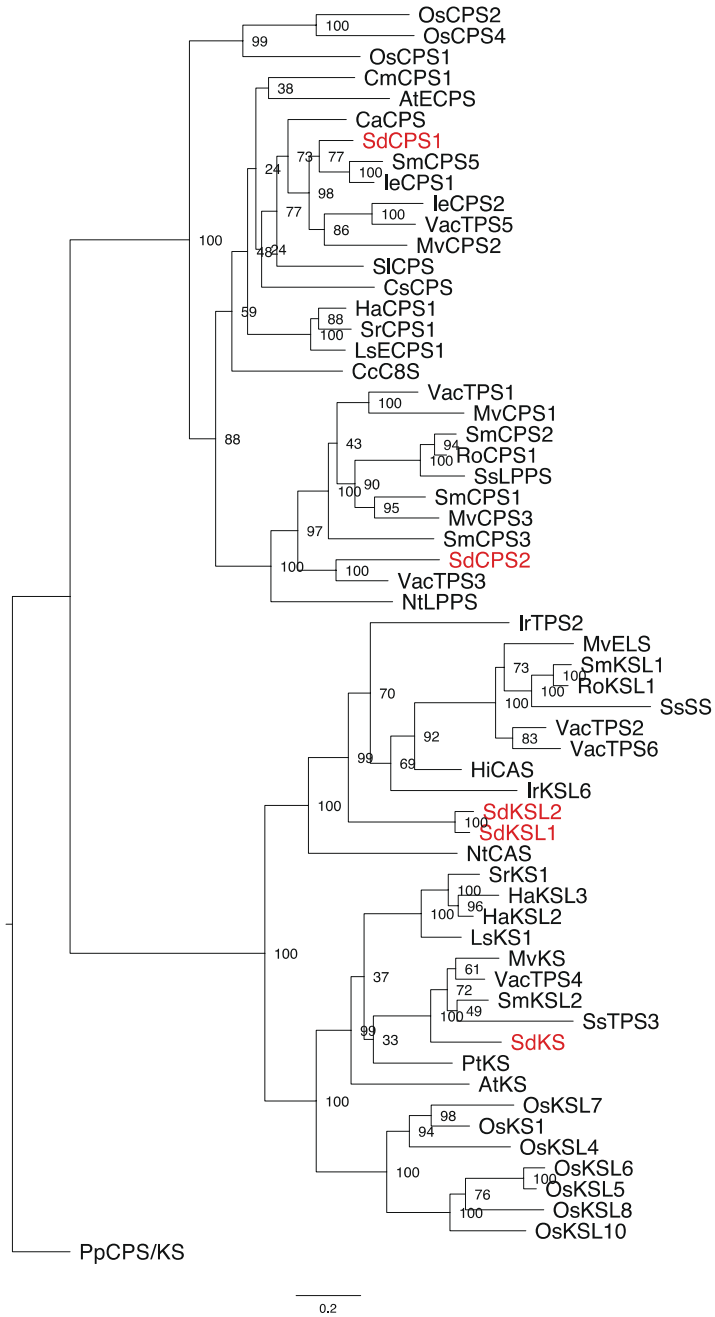

Figure 1. Phylogenetic trees of diterpene synthases. The maximum likelihood trees illustrates the phylogenetic relatedness of *S. dulcis* DTSs with other DTSs. The ancestral *Physcomitrella patens ent*-kaurene synthase (PpCPS/KS) was used to root the tree. Bootstrap values are displayed next to the nodes. Descriptions of DTSs used in the phylogeny are listed in Table S2.

2.2. Characterization of Enzymic Function of DTSs

In order to characterize the enzymatic function of SdCPS2, cDNA was truncated to remove signal-sequence targeting for the plastid, and then ligated into the pSdGG vector to construct pSdGG/SdCPS2 plasmid. This plasmid harbors GGPP synthase from *S. dulcis* to provide the substrate GGPP for SdCPS2 in recombinant *E. coli*. So far, transit-peptide sequences have been shown to interfere functionally with the expression of diterpene synthases; therefore, we truncated the corresponding nucleotide sequences to construct the recombinant cells. Together with the construct, transformants with pSdGG/SdCPS1 (*ent*-CPS from *S. dulcis*), pSdGG/SmCPS1 (*normal*-CPS from *Salvia miltiorrhiza*) [10] or pSdGG/OsCPS4 (*syn*-CPS from *Oryza sativa*) [11] were prepared in order to compare the enzymatic reaction products. The recombinant cells were cultured in the Terrific-broth liquid media, supplemented with 1% glucose and induced with 0.5 mM IPTG. After 72 h incubation at 16 °C, the medium was extracted twice with *n*-hexane, and then the extract was concentrated and analyzed using GC-MS. In our assay system, we confirmed that diterpene alcohols as dephosphorylated products were secreted to culture media from host cells.

E. coli harboring pSdGG/SdCPS2 produced a single diterpene hydrocarbon as peak **3′** (Figure 2A), and its retention time and mass spectra were identical with that derived from OsCPS4 (Figure 2B). In addition, different retention times of the enzymatic products **5′** (Figure 2C) and **6′** (Figure 2D) were observed in the case of SdCPS1 (*ent*-CPS) and SmCPS1 (*normal*-CPS), respectively. Therefore, SdCPS2 was judged not to be *ent*- or *normal*-CPS. To provide further evidence for the identity of the SdCPS2 product, the diterpene alcohol derivative was isolated using silica gel column chromatography and applied to the NMR analyses (Figures S2–S5). As a result, its structure was found to be identical to a *syn*-copalol, based on the comparison data from the ^{1}H- and ^{13}C-NMR chemical shifts (Table S3) [12]. However, it is impossible to separate enantiomers such as *syn*-copalol and *syn-ent*-copalol on the GC-MS equipped with an achiral-phase capillary column, and we were not able to achieve fine separation using chiral GC (data not shown). For this reason, we chose to utilize a known enzyme (OsKSL4) for cyclization from *syn*-CPP to *syn*-pimara-7,11-diene (**7**) [13]. Recombinant *E. coli* transformed with pSdGG/SdCPS2 and pOsKSL4 was cultured and treated with IPTG to produce **7,** as shown in Figure 2E. The retention time and mass spectrum were identical to those produced by the recombinant *E. coli* transformed with pSdGG/OsCPS4 and pOsKSL4 (Figure 2F). This indicated that the enzymic-reaction products of SdCPS2 could be cyclized by OsKSL4, whose substrate is a *syn*-copalyl diphosphate. Therefore, our cloned SdCPS2 was found to be a *syn*-CPS.

Subsequently, pSdKSL1 and pSdKSL2mut were constructed, and transformed with pSdGG/SdCPS2 into *E. coli* cells to elucidate the function of both DTSs. As described above, *SdKSL2* contained a non-sense mutation in its CDS. By comparing the nucleotide sequences of *SdKSL1* and *SdKSL2*, we introduced a mutation (A682G) to recover its enzymatic function (*SdKSL2mut*). As shown in Figure 3A, peak **4′** appeared together with peak **3′**, which corresponded to a *syn*-copalol. The mass spectrum of peak **4′** revealed that the corresponding compound was suggested to be a novel diterpene alcohol, synthesized by SdKSL1. In order to identify this enzymatic-reaction, product **4** was isolated using silica gel column chromatography from large-scale culture. NMR analyses (Figures S6–S10), including 2D experiments of **4,** revealed that it was identical to scopadula-13α-ol (demalonyl thyrsiflorin A) (Table S4) [14]. Therefore, SdKSL1 could be regarded as a novel class I DTS, scopadula-13α-ol synthase. On the other hand, SdKSL2mut was able to produce different diterpene hydrocarbons, as shown in Figure 3B. The mass spectrum of peak **8** was identical to that of a previously reported aphidicol-16-ene [13,15]. In order to confirm its chemical structure, we purified it using silica gel column chromatography, and applied it to NMR analyses (Figures S11–S16). The ^{1}H and ^{13}C NMR chemical shifts of **8** were identified as an aphidicol-16-ene (Table S5).

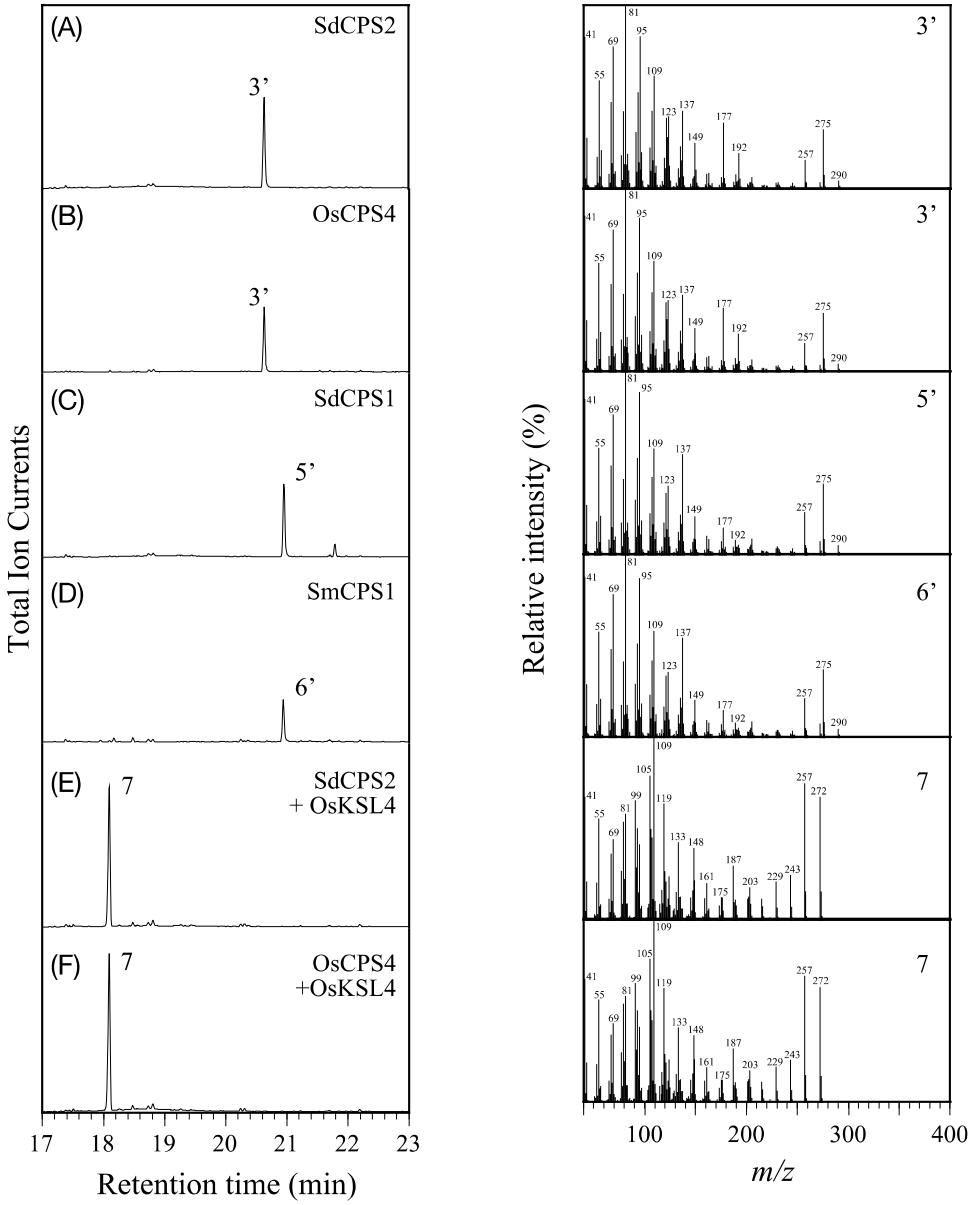

Figure 2. GC-MS analyses of extracts from cultures expressing the indicated gene products. Shown are total-ion-count (TIC) chromatograms on the left, and mass spectra for the indicated peak on the right. (**A**) Production of **3** by SdCPS2, observed as the dephosphorylated derivative *syn*-copalol (**3′**) produced by endogenous phosphatases. (**B**) Production of **3** by OsCPS4, observed as the dephosphorylated derivative *syn*-copalol (**3′**) produced by endogenous phosphatases. (**C**) Production of **5** by SdCPS1, observed as the dephosphorylated derivative *ent*-copalol (**5′**) produced by endogenous phosphatases. (**D**) Production of **6** by SmCPS1, observed as the dephosphorylated derivative *normal*-copalol (**6′**) produced by endogenous phosphatases. (**E**) Production of **7** by SdCPS2 and OsKSL4. (**F**) Production of **7** by OsCPS4 and OsKSL4.

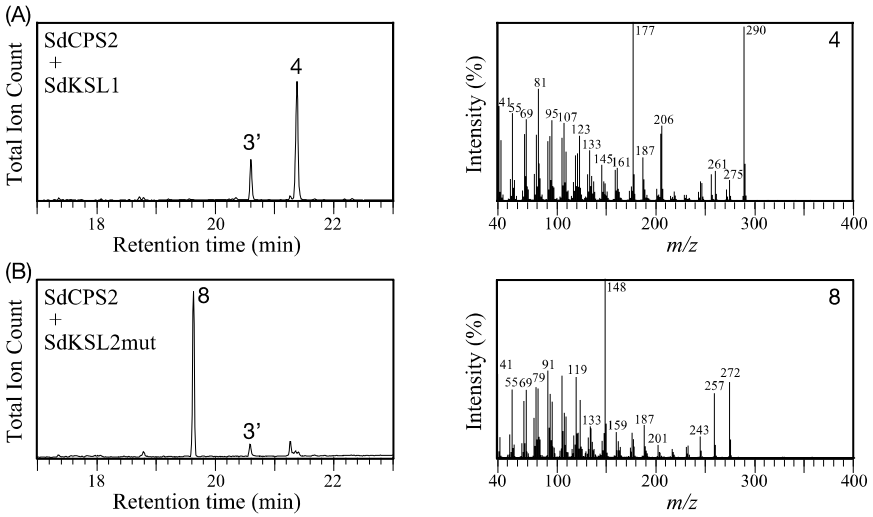

Figure 3. GC-MS analyses of extracts from cultures expressing the indicated gene products. Shown are the total-ion-count (TIC) chromatograms on the left, and mass spectra for the indicated peak on the right. (**A**) Production of **4** (scopadula-13α-ol) by SdCPS2 and SdKSL1. (**B**) Production of **8** (aphidicol-16-ene) by mutated SdKSL2mut.

2.3. Quantification of Scopadulcic Acid B (1) and Realtime qPCR Analysis of SdCPS2 and SdKSL1

As described above, *SdCPS2* and *SdKSL1* were suggested to be involved in the biosynthesis of unique tetracyclic diterpenes in *S. dulcis*. Therefore, we analyzed the amounts of scopadulcic acid B (**1**) and the expression levels of those transcripts in plant tissues. As shown in Figure 4A, scopadulcic acid B (**1**) accumulated in the young leaf. Similarly, the highest expression levels of *SdCPS2* and *SdKSL1* were observed in the young leaf (Figure 4B).

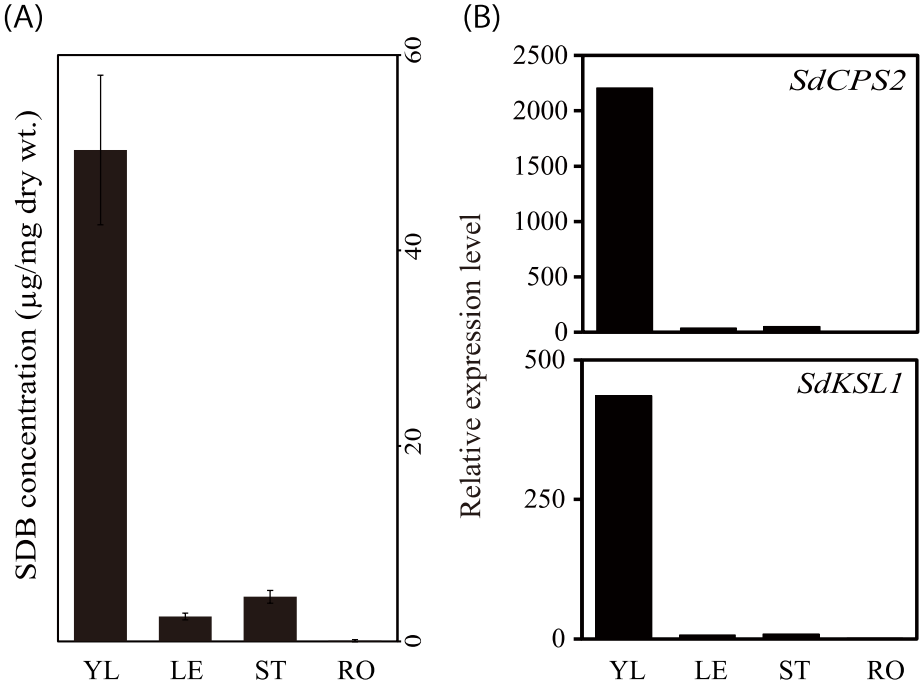

Figure 4. Quantification of SDB production and qRT-PCR analysis of the expression level of *SdCPS2* and *SdKSL1* in *S. dulcis* tissues. (**A**) Quantification of scopadulcic acid B (**1**) by HPLC in *S. dulcis* tissues. YL: young leaf, LE: leaf, ST: stem, and RO: root. (**B**) The 18S rRNA gene was used for normalization. The transcript level of each gene in the root was set to 1.0.

3. Discussion

In this report, we discovered three diterpene synthases responsible for the unique tetracyclic diterpene biosynthesis in *S. dulcis*. Reaction mechanisms of SdKSL1 and SdKSL2 are proposed, as shown in Scheme 2. At first, the lysis of the allylic diphosphate ester in **3** induces type A cyclization, initiated by the formation of an allylic cation, followed by *si*-face attack of the olefin, which is accompanied by a hydride shift from C-9 to C-8 to afford the 8β-pimarenyl cation (**10**) [5]. The carbocation is suggested to cyclize with the vinyl group to give **11**, and rearrangement of **11** provides secondary cation **13,** via tertiary cation **12**. This undergoes trapping with the nucleophilic oxygen of water, to give tetracyclic diterpene alcohol **4**. On the other hand, SdKSL2 is suggested to produce an aphidicol-16-ene (**8**). *S. dulcis* has been reported to produce an aphidicolane-type diterpene, scopadulin [16]. Thus, the functionally active SdKSL2-related enzyme may be involved in the biosynthesis of scopadulin.

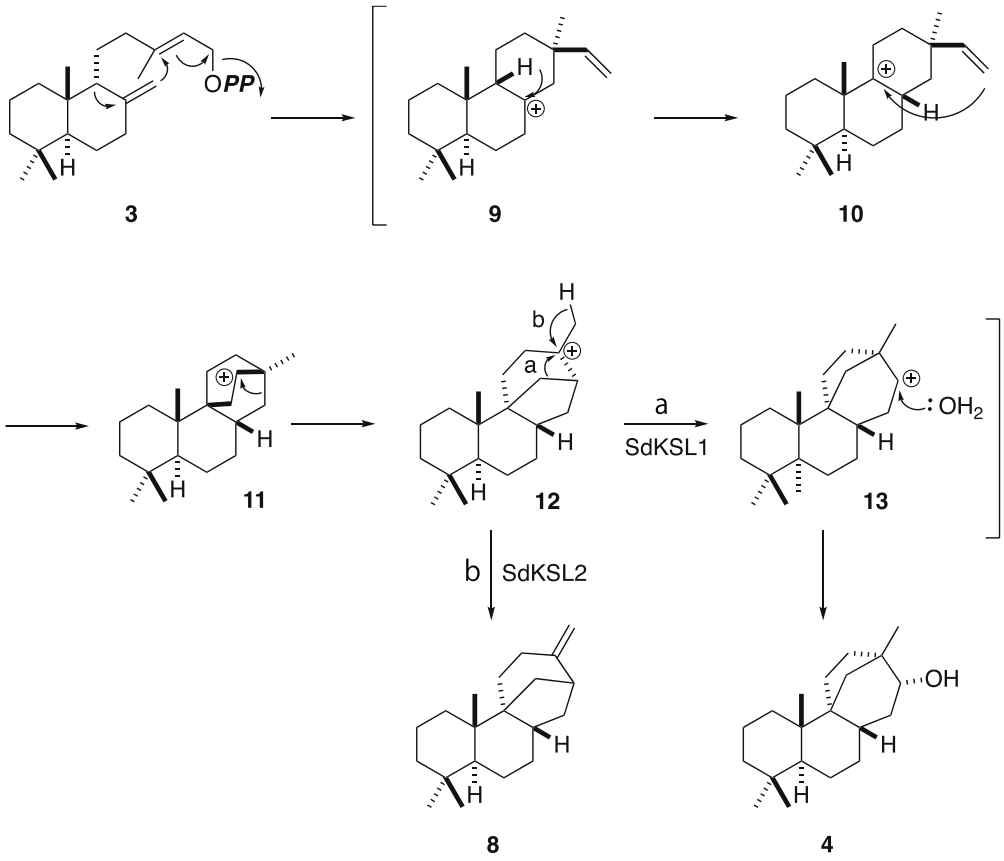

Scheme 2. Proposed enzymatic formation of scopadula-13a-ol (**4**) and aphidicol-16-ene (**8**).

Figure 4 reveals that the preserved tissue, i.e., young leaf, of scopadulcic acid B (**1**) corresponded to the expression levels of *SdCPS2* and *SdKSL1*. The data might strongly support these two DTSs being involved in the unique diterpene biosynthesis.

In conclusion, it is shown here that SdCPS2 and SdKSL1 exhibit class II and class I diterpene synthase activities, respectively. The former catalyze the formation from **2** to **3**, and the later cyclize **3** to **4**; therefore, SdCPS2 and SdKSL1 were regarded as *syn*-CPS and scopadula-13α-ol synthase, respectively. So far, two *syn*-CPSs, OsCPS4 and VacTPS3, have been reported, whereas this paper is the first to report the unique tetracyclic diterpene cyclase, SdKSL1. Although **4** was not isolated from natural sources, a structurally related one, thyrsiflorin A, was isolated from *Calceolaria thyrsiflora*. During structural elucidation, demalonyl thyrsiflorin A was reported, and it was found that the compound was identical to **4**. Recently, **4** has been reported to have cytotoxic effects on melanoma cells [17] and

inducible effects on apoptosis and necrosis in the human cancer cell-line [18]. In these papers, **4** was prepared by the reduction of naturally occurring thyrsiflorin A. Therefore, the cloned enzymes described in this study, under large-scale fermentation production could provide a way to produce **4** for further evaluation of its biological effects.

4. Material and Methods

4.1. Plant Material

Scoparia dulcis was germinated under sterile conditions and was grown on half-strength Murashige and Skoog agar medium at 25 °C, under continuous illumination. After 5–6 weeks of growth, the seedlings were harvested, frozen immediately in liquid nitrogen, and stored at −80 °C for RNA isolation.

4.2. Cloning of Diterpene Synthases

The total RNA was isolated from the seedlings using TRIzol reagent (Invitrogen, Carlsbad, CA, USA) and cDNA was generated by the reverse-transcription reaction, using the PrimeScript II First-strand cDNA synthesis kit (Takara Bio Inc., Kusatsu, Shiga, Japan). The *SdCPS2*, *SdKSL1*, and *SdKSL2* genes were cloned, using the primers described.

4.3. Construction of Expression Vectors

All expression vectors were constructed according to the method previously reported by Cyr et al. [19]. Briefly, *SdGGPPS* (Accession No. AB034250) was truncated, to remove the transit-peptide sequence (57 amino acids), and introduced into the pACYC-Duet (Novagen Merck, Darmstadt, Germany) multiple cloning site 2 (MCS2). The ORF of *SdCPS2*, after the transit-peptide sequence was truncated, was then cloned into the MCS1 of the vector, using the corresponding *Nco*I and *Not*I restriction site to construct pSdGG/SdCPS2. Similarly, *SdCPS1* (Accession No. AB169881), *SmCPS1* (Accession No. KC814639), and *OsCPS4* (Accession No. BAD42451) were cloned into MCS1, to give pSdGG/SdCPS1, pSdGG/SmCPS1, and pSdGG/OsCPS4 vectors, respectively. *SdKSL1* or *OsKSL4* (Accession No. Q0JEZ8) were cloned into the multiple cloning site in pET28b (Novagen Merck), using the corresponding *Nco*I and *Not*I restriction site, to give pSdKSL1 or pOsKSL4 plasmids. The *SdKSL2* contained the stop codon.

4.4. Heterologous Expression and Metabolite Analysis

The resulting constructs were transformed into the C41 strain of *E. coli* (Lucigen), and heterologously expressed. These recombinants were grown in liquid TB media (12 g casein, 24 g yeast extract, 8 mL 50% glycerol in 1 L H_2O, and pH adjusted to 7.0) with the appropriate antibiotics at 37 °C to OD_{600}~0.6, then transferred to 16 °C for an hour and induced with IPTG (0.5 mM final concentration). After 24 h growth at 16 °C, the dephosphorylated enzymatic products were extracted with *n*-hexane (equal volume). The organic layer was separated out and then dried under N_2, with the residue re-suspended in fresh hexanes and analyzed using GC-MS. Note that dephosphorylation of the class II diterpene synthase products, **3**, **5**, and **6**, to generate **3′**, **5′**, and **6′** are mediated by the endogenous phosphatases in *E. coli* as described elsewhere [20]. GC-MS analysis was carried out using a DB-5MS fused-silica capillary column (Agilent) on a Shimadzu QP-2010 *Ultra* gas chromatograph mass spectrometer in electro-ionization mode (70 eV). Each sample was injected at 230 °C in the splitless mode. The samples were initially held at 50 °C for 1 min, following which the oven temperature was increased by 10 °C/min to 300 °C and held for 5 min. The flow rate of He carrier gas was set at 1.9 mL/min. The MS data were collected from 40 to 400 *m/z*.

4.5. Phylogenetic Analyses

Phylogenetic analyses were performed using RAxML software [21] with alignments prepared using the MAFFT program. Selected DTS proteins were aligned by employing a highly accurate method: L-INS-I. The substitution model was selected according to the

maximum AIC, as determined by ModelTest-NG [22]. Maximum-likelihood (ML) trees were built, using the JTT+I+G4+F model and 1000 replicates of the bootstrap analyses, and the obtained phylogeny was displayed using FigTree software (http://tree.bio.ed.ac.uk/software/figtree) (accessed on 18 November 2018).

4.6. Quantifation of Scopadulcic Acid B

The quantification of scopadulcic acid B was performed, using the previously reported method [23]. Briefly, 1 mL of $CHCl_3$:MeOH (3:1) solution was added to the freeze-dried young leaf (YL), mature leaf (LE), stem (ST), and root (RO) (approximately 20 mg) of *S. dulcis*, and the mixture was sonicated for 20 min. After centrifugation at 13,000 rpm for 10 min, 1 mL of distilled water was added to the supernatant, and the mixture was vigorously shaken at room temperature for 30 min. After centrifugation at 13,000 rpm for 10 min, 0.6 mL of the lower layer ($CHCl_3$ layer) was dried in vacuo. The residue was dissolved with 1 mL of MeOH and quantified using the HPLC system (Hitachi, D7000 system) equipped with a Cosmosil C18ARII column (Nacalai Inc., Kyoto, Japan).

4.7. Real-Time qPCR Analysis

Real-time qPCR was performed using Brilliant III Ultra-Fast SYBR Green QPCR Master Mix with ROX (Agilent Technologies, Santa Clara, CA, USA) on an AriaMX real-time QPCR system (Agilent Technologies). The *S. dulcis* 18S rRNA gene was used for normalization. The primer sequences used in the qPCR study are listed in Table S1. Calibration curves were produced for each of the primer pairs, and quantification was performed using the Agilent AriaMx software (Agilent Technologies, ver.1.8). Each sample was tested three times.

Supplementary Materials: The following supporting information can be downloaded at: https://www.mdpi.com/article/10.3390/plants12010069/s1, Figure S1: Amino acid alignments of DTSs from *S. dulcis*; Figure S2: ^{1}H NMR spectrum of *syn*-copalol (**3′**) in $CDCl_3$, Figure S3: ^{13}C NMR spectrum of *syn*-copalol (**3′**) in $CDCl_3$; Figure S4: HMQC spectrum of *syn*-copalol (**3′**) in $CDCl_3$; Figure S5: HMBC spectrum of *syn*-copalol (**3′**) in $CDCl_3$; Figure S6: ^{1}H NMR spectrum of scopadula-13a-ol (**4**) in $CDCl_3$; Figure S7: ^{13}C NMR spectrum of scopadula-13a-ol (**4**) in $CDCl_3$; Figure S8: COSY spectrum of scopadula-13a-ol (**4**) in $CDCl_3$; Figure S9: HMQC spectrum of scopadula-13a-ol (**4**) in $CDCl_3$; Figure S10: HMBC spectrum of scopadula-13a-ol (**4**) in $CDCl_3$; Figure S11: ^{1}H NMR spectrum of aphidicol-16-ene (**8**) in $CDCl_3$; Figure S12: ^{13}C NMR spectrum of aphidicol-16-ene (**8**) in $CDCl_3$; Figure S13: COSY spectrum of aphidicol-16-ene (**8**) in $CDCl_3$; Figure S14: HMQC spectrum of aphidicol-16-ene (**8**) in $CDCl_3$; Figure S15: HMBC spectrum of aphidicol-16-ene (**8**) in $CDCl_3$; Figure S16: NOESY spectrum of aphidicol-16-ene (**8**) in $CDCl_3$; Table S1: Primers used in the present study; Table S2: Abbreviations and accession numbers of DTSs, References [24–43] are cited in the supplementary materials; Table S3: ^{1}H and ^{13}C NMR assignments of *syn*-copalol (**3′**) in $CDCl_3$; Table S4: ^{1}H and ^{13}C NMR assignments of scopadula-13a-ol (**4**) in $CDCl_3$; Table S5: ^{1}H and ^{13}C NMR assignments of aphidicol-16-ene (**8**) in $CDCl_3$.

Author Contributions: Conceptualization, J.-B.L. and Y.Y.; methodology and software, J.-B.L. and Y.Y.; investigation, J.-B.L., T.O. and Y.Y.; writing—original draft preparation, J.-B.L.; writing—review and editing, J.-B.L. and Y.Y., project administration, J.-B.L. and Y.Y.; funding acquisition, Y.Y. All authors have read and agreed to the published version of the manuscript.

Funding: This study was financially supported by Grant-in-Aid for Scientific Research C (18K06729) from the Ministry of Education, Culture, Sports, Science, and Technology of Japan.

Data Availability Statement: The data contained within the present article and in its Supplementary Materials are freely available upon request to the corresponding author.

Acknowledgments: *O. sativa* L. cv. *Nipponbare* seed was a generous gift from the Agricultural Research Institute, Toyama Prefectural Agricultural, Forestry & Fisheries Research Center. We thank Io Umebara for technical assistance.

Conflicts of Interest: The authors declare no conflict of interest.

References

1. Hayashi, T.; Kishi, M.; Kawasaki, M.; Arisawa, M.; Shimizu, M.; Shoichi, S.; Yoshizaki, M.; Tezuka, Y.; Kikuchi, T.; Berganza, L.H.; et al. Scopadulcic Acid-A and -B, New Diterpenoids with a Novel Skeleton, from a Paraguayan Crude Drug "Typychá Kuratũ" (*Scoparia Dulcis* L.). *Tetrahedron Lett.* **1987**, *28*, 3693–3696. [CrossRef]
2. Mafu, S.; Zerbe, P. Plant Diterpenoid Metabolism for Manufacturing the Biopharmaceuticals of Tomorrow: Prospects and Challenges. *Phytochem. Rev.* **2017**, *330*, 70. [CrossRef]
3. Peters, R.J. Two Rings in Them All: The Labdane -Related Diterpenoids. *Nat. Prod. Rep.* **2010**, *27*, 1521–1530. [CrossRef] [PubMed]
4. Yamamura, Y.; Kurosaki, F.; Lee, J.-B. Elucidation of Terpenoid Metabolism in Scoparia Dulcis by RNA-Seq Analysis. *Sci. Rep.* **2017**, *7*, 43311. [CrossRef]
5. Christianson, D.W. Structural and chemical biology of terpenoid cyclases. *Chem. Rev.* **2017**, *117*, 11570–11648. [CrossRef]
6. Heskes, A.M.; Sundram, T.C.M.; Boughton, B.A.; Jensen, N.B.; Hansen, N.L.; Crocoll, C.; Cozzi, F.; Rasmussen, S.; Hamberger, B.; Hamberger, B.; et al. Biosynthesis of Bioactive Diterpenoids in the Medicinal Plant Vitex Agnus-Castus. *Plant J.* **2018**, *93*, 943–958. [CrossRef]
7. Otomo, K.; Kenmoku, H.; Oikawa, H.; König, W.A.; Toshima, H.; Mitsuhashi, W.; Yamane, H.; Sassa, T.; Toyomasu, T. Biological functions of *ent*- and *syn*-copalyl diphosphate synthase in rice: Key enzymes for the branch point of gibberellin and phytoalexin biosynthesis. *Plant J.* **2004**, *39*, 886–893. [CrossRef]
8. Jin, B.; Cui, G.; Guo, J.; Tang, J.; Duan, L.; Lin, H.; Shen, Y.; Chen, T.; Zhang, H.; Huang, L. Functional diversification of kaurene synthase-like genes in *Isodon rubescens*. *Plant Physiol.* **2017**, *174*, 943–955. [CrossRef]
9. Pelot, K.A.; Hagelthorn, D.M.; Addison, J.B.; Zerbe, P. Biosynthesis of the oxygenated diterpene nezukol in the medicinal plant *Isodon rubescens* is catalyzed by a pair of diterpene synthases. *PLoS ONE* **2017**, *12*, e0176507. [CrossRef]
10. Ma, Y.; Yuan, L.; Wu, B.; Li, X.; Chen, S.; Lu, S. Genome-Wide Identification and Characterization of Novel Genes Involved in Terpenoid Biosynthesis in Salvia Miltiorrhiza. *J. Exp. Bot.* **2012**, *63*, 2809–2823. [CrossRef]
11. Xu, M.; Hillwig, M.L.; Prisic, S.; Coates, R.M.; Peters, R.J. Functional Identification of Rice Syn-Copalyl Diphosphate Synthase and Its Role in Initiating Biosynthesis of Diterpenoid Phytoalexin/Allelopathic Natural Products. *Plant J.* **2004**, *39*, 309–318. [CrossRef] [PubMed]
12. Toshima, H.; Oikawa, H.; Yada, H.; Ono, H.; Toyomasu, T.; Sassa, T. Total Synthesis of (±)-Syn-Copalol. *Biosci. Biotechnol. Biochem.* **2002**, *66*, 2504–2510. [CrossRef] [PubMed]
13. Morrone, D.; Jin, Y.; Xu, M.; Choi, S.-Y.; Coates, R.M.; Peters, R.J. An Unexpected Diterpene Cyclase from Rice: Functional Identification of a Stemodene Synthase. *Arch. Biochem. Biophys.* **2006**, *448*, 133–140. [CrossRef] [PubMed]
14. Chamy, M.C.; Piovano, M.; Garbarino, J.A.; Miranda, C. Diterpenoids from Calceolaria Thyrsiflora. *Phytochemistry* **1991**, *30*, 589–592. [CrossRef]
15. Oikawa, H.; Toyomasu, T.; Toshima, H.; Ohashi, S.; Kawaide, H.; Kamiya, Y.; Ohtsuka, M.; Shinoda, S.; Mitsuhashi, W.; Sassa, T. Cloning and Functional Expression of CDNA Encoding Aphidicolan-16β-Ol Synthase: A Key Enzyme Responsible for Formation of an Unusual Diterpene Skeleton in Biosynthesis of Aphidicolin. *J. Am. Chem. Soc.* **2001**, *123*, 5154–5155. [CrossRef]
16. Hayashi, T.; Kawasaki, M.; Miwa, Y.; Taga, T.; Morita, N. Antiviral agents of plant origin III.: Scopadulin, a novel tetracyclic diterpene from *Scoparia dulcis*. *Chem. Pharm. Bull.* **1990**, *38*, 945–947. [CrossRef]
17. Cardile, V.; Avola, R.; Graziano, A.C.E.; Piovano, M.; Russo, A. Cytotoxicity of Demalonyl Thyrsiflorin A, a Semisynthetic Labdane-Derived Diterpenoid, to Melanoma Cells. *Toxicol Vitr.* **2018**, *47*, 274–280. [CrossRef]
18. Garbarino, J.A.; Cardile, V.; Lombardo, L.; Chamy, M.C.; Piovano, M.; Russo, A. Demalonyl Thyrsiflorin A, a Semisynthetic Labdane-Derived Diterpenoid, Induces Apoptosis and Necrosis in Human Epithelial Cancer Cells. *Chem.-Biol. Interact* **2007**, *169*, 198–206. [CrossRef]
19. Cyr, A.; Wilderman, P.R.; Determan, M.; Peters, R.J. A Modular Approach for Facile Biosynthesis of Labdane-Related Diterpenes. *J. Am. Chem. Soc.* **2007**, *129*, 6684–6685. [CrossRef]
20. Xu, M.; Jia, M.; Hong, Y.J.; Yin, X.; Tantillo, D.J.; Proteau, P.J.; Peters, R.J. Premutilin Synthase: Ring Rearrangement by a Class II Diterpene Cyclase. *Org. Lett.* **2018**, *20*, 1200–1202. [CrossRef]
21. Kozlov, A.M.; Darriba, D.; Flouri, T.; Morel, B.; Stamatakis, A. RAxML-NG: A Fast, Scalable, and User-Friendly Tool for Maximum Likelihood Phylogenetic Inference. *Bioinformatics* **2019**, *35*, 4453–4455. [CrossRef] [PubMed]
22. Darriba, D.; Posada, D.; Kozlov, A.M.; Stamatakis, A.; Morel, B.; Flouri, T. ModelTest-NG: A New and Scalable Tool for the Selection of DNA and Protein Evolutionary Models. *Mol. Biol. Evol.* **2019**, *37*, 291–294. [CrossRef] [PubMed]
23. Nkembo, M.K.; Kurosaki, F.; Lee, J.-B.; Hayashi, T. Stimulation of calcium signal transduction results in enhancement of production of scopadulcic acid B by methyl jasmonate in the cultured tissues of *Scoparia dulcis*. *Plant. Biotechnol.* **2005**, *22*, 333–337. [CrossRef]
24. Mayer, K.; Schüller, C.; Wambutt, R.; Murphy, G.; Volckaert, G.; Pohl, T.; Düsterhöft, A.; Stiekema, W.; Entian, K.D.; Terryn, N.; et al. Sequence and analysis of chromosome 4 of the plant Arabidopsis thaliana. *Nature* **1999**, *402*, 769–777. [CrossRef] [PubMed]
25. Theologis, A.; Ecker, J.R.; Palm, C.J.; Federspiel, N.A.; Kaul, S.; White, O.; Alonso, J.; Altafi, H.; Araujo, R.; Bowman, C.L.; et al. Sequence and analysis of chromosome 1 of the plant Arabidopsis thaliana. *Nature* **2000**, *408*, 816–820. [CrossRef]
26. Falare, V.; Pichersky, E.; Kanellis, A.K. A copal-8-ol diphosphate synthase from the angiosperm *cistus creticus* subsp. Criticus is a putative key enzyme for the formation of pharmacologically active, oxygen-containing labdane-type diterpenes. *Plant Physiol.* **2010**, *154*, 301–310. [CrossRef]

27. Pugliesi, C.; Fambrini, M.; Salvini, M. Molecular cloning and expression profile analysis of three sunflower (*Helianthus annuus*) diterpene synthase genes. *Biochem. Genet.* **2011**, *49*, 46–62. [CrossRef]
28. Li, J.; Chen, Q.; Jin, Q.; Gao, J.; Zhao, P.; Lu, S.; Zeng, Y. IeCPS2 is potentially involved in the biosynthesis of pharmacologically active Isodon diterpenoids rather than gibberellin. *Phytochemistry* **2012**, *76*, 32–39. [CrossRef]
29. Sawada, Y.; Katsumata, T.; Kitamura, J.; Kawaide, H.; Nakajima, M.; Asami, T.; Nakaminami, K.; Kurahashi, T.; Mitsuhashi, W.; Inoue, Y.; et al. Germination of photoblastic lettuce seeds is regulated via the control of endogenous physiologically active gibberellin content, rather than of gibberellin responsiveness. *J. Exp. Bot.* **2008**, *59*, 3383–3393. [CrossRef]
30. Zerbe, P.; Chiang, A.; Dullat, H.; O'Neil-Johnson, M.; Starks, C.; Hamberger, B.; Bohlmann, J. Diterpene synthases of the biosynthetic system of medicinally active diterpenoids in Marrubium vulgare. *Plant J.* **2014**, *79*, 914–927. [CrossRef]
31. Sallaud, C.; Giacalone, C.; Töpfer, R.; Goepfert, S.; Bakaher, N.; Rösti, S.; Tissier, A. Characterization of two genes for the biosynthesis of the labdane diterpene Z-abienol in tobacco (*Nicotiana tabacum*) glandular trichomes. *Plant J.* **2012**, *72*, 1–17. [CrossRef] [PubMed]
32. Kawahara, Y.; de la Bastide, M.; Hamilton, J.P.; Kanamori, H.; McCombie, W.R.; Ouyang, S.; Schwartz, D.C.; Tanaka, T.; Wu, J.; Zhou, S.; et al. Improvement of the Oryza sativa Nipponbare reference genome using next generation sequence and optical map data. *Rice* **2013**, *6*, 4. [CrossRef] [PubMed]
33. Margis-Pinheiro, M.; Zhou, X.; Zhu, Q.; Dennis, E.S.; Upadhyaya, N.M. Isolation and characterization of a Ds-tagged rice (*Oryza sativa* L.) GA-responsive dwarf mutant defective in an early step of the gibberellin biosynthesis pathway. *Plant Cell Rep.* **2005**, *23*, 819–833. [CrossRef] [PubMed]
34. Rice Full-Length cDNA Consortium. Collection, mapping, and annotation of over 28,000 cDNA clones from japonica rice. *Science* **2003**, *301*, 376–379. [CrossRef] [PubMed]
35. Brückner, K.; Bozic, D.; Manzano, D.; Papaefthimiou, D.; Pateraki, I.; Scheler, U.; Ferrer, A.; de Vos, R.C.H.; Kanellis, A.K.; Tissier, A. Characterization of two genes for the biosynthesis of abietane-type diterpenes in rosemary (*Rosmarinus officinalis*) glandular trichomes. *Phytochemistry* **2014**, *101*, 52–64. [CrossRef] [PubMed]
36. Nakagiri, T.; Lee, J.-B.; Hayashi, T. cDNA cloning, functional expression and characterization of ent-copalyl diphosphate synthase from *Scoparia dulcis* L. *Plant Sci.* **2005**, *169*, 760–767. [CrossRef]
37. Yamamura, Y.; Taguchi, Y.; Ichitani, K.; Umebara, I.; Ohshita, A.; Kurosaki, F.; Lee, J.-B. Characterization of ent-kaurene synthase and kaurene oxidase involved in gibberellin biosynthesis from Scoparia dulcis. *J. Nat. Prod.* **2018**, *72*, 456–463. [CrossRef]
38. Cui, G.; Duan, L.; Jin, B.; Qian, J.; Xue, Z.; Shen, G.; Snyder, J.H.; Song, J.; Chen, S.; Huang, L.; et al. Functional divergence of diterpene synthases in the medicinal plant Salvia miltiorrhiza. *Plant Physiol.* **2015**, *169*, 1607–1618. [CrossRef]
39. Gao, W.; Hillwig, L.H.; Huang, L.; Cui, G.; Wang, X.; Kong, J.; Yang, B.; Peters, R.J. A functional genomics approach to tanshinone biosynthesis provides stereochemical insights. *Org. Lett.* **2009**, *11*, 5170–5173. [CrossRef]
40. Richman, A.S.; Gijzen, M.; Starratt, A.N.; Yang, Z.; Brandle, J.E. Diterpene synthesis in Stevia rebaudiana: Recruitment and up-regulation of key enzymes from the gibberellin biosynthetic pathway. *Plant J.* **1999**, *19*, 411–421. [CrossRef]
41. Schalk, M.; Pastore, L.; Mirata, M.A.; Khim, S.; Schouwey, M.; Deguerry, F.; Pineda, V.; Rocci, L.; Daviet, L. Toward a biosynthetic route to sclareol and amber odorants. *J. Am. Chem. Soc.* **2012**, *134*, 18900–18903. [CrossRef] [PubMed]
42. Caniard, A.; Zerbe, P.; Legrand, S.; Cohade, A.; Valot, N.; Magnoard, J.L.; Bohlmann, J.; Legendre, L. Discovery and functional characterization of two diterpene synthases for sclareol biosynthesis in *Salvia sclarea* (L.) and their relevance for perfume manufacture. *BMC Plant Biol.* **2012**, *12*, 119. [CrossRef] [PubMed]
43. Hayashi, K.; Kawaide, H.; Notomi, M.; Sakigi, Y.; Matsuo, A.; Nozaki, H. Identification and functional analysis of bifunctional ent-kaurene synthase from the moss Physcomitrella patens. *FEBS Lett.* **2006**, *580*, 6175–6181. [CrossRef] [PubMed]